

# On the Existence of Steady States for Blended Gas Flow with Non-Constant Compressibility Factor on Networks

S. Göttlich<sup>1</sup>, M. Schuster<sup>2</sup>, A. Ulke<sup>1</sup>

**Abstract** In this paper, we study hydrogen-natural gas mixtures transported through pipeline networks. The flow is modeled by the isothermal Euler equations with a pressure law involving a non-constant, composition-dependent compressibility factor. For a broad class of such compressibility models, we prove the existence of steady-state solutions on networks containing compressor stations. The analysis is based on an implicit representation of the pressure profiles and a continuity argument that overcomes the discontinuous dependence of the gas composition on the flow direction. Numerical examples illustrate the influence of different compressibility models on the resulting states.

## 1 Introduction and Motivation

The ongoing transformation of the global energy system towards climate neutrality has placed hydrogen at the center of scientific and industrial discussions. As an energy carrier, hydrogen possesses several highly attractive properties. It can be produced from renewable energy sources such as wind or solar power, and its use does not generate carbon dioxide emissions, releasing only water and heat [8, 11]. Moreover, hydrogen is regarded as a key enabler for the decarbonization of sectors that cannot be easily electrified, including parts of heavy industry and long-distance transport. In addition, hydrogen provides flexibility within the energy system by enabling large-scale energy storage and sector coupling [11, 33], which underlines hydrogen’s anticipated relevance in future energy infrastructures.

Despite its promising potential, hydrogen will not immediately replace natural gas as a primary energy source. Instead, a gradual integration into existing infrastructures is currently considered the most feasible pathway. In this context, blending hydrogen into natural gas pipeline networks has emerged as a pragmatic transition strategy, allowing for a reduction in greenhouse gas emissions while relying on well-established transport systems. Large-scale hydrogen transport networks are already under development worldwide, cf. [12] for Europe, [25] for Asia, and [34] for the United States. Nevertheless, for the foreseeable future, hydrogen-natural gas mixtures are expected to dominate practical applications rather than pure hydrogen flows.

The safe and efficient operation of pipeline networks carrying hydrogen-enriched natural gas requires a detailed mathematical understanding of the underlying flow processes. While the transport of pure natural gas (or any other single gas) can be accurately described by the isothermal Euler equations, cf. [3, 9, 16, 24]:

$$\partial_t \rho_{\text{NG}}(t, x) + \partial_x q_{\text{NG}}(t, x) = 0, \quad (1.1a)$$

$$\partial_t q_{\text{NG}}(t, x) + \partial_x \left[ p_{\text{NG}}(\rho_{\text{NG}}(t, x)) + \frac{q_{\text{NG}}^2(t, x)}{\rho_{\text{NG}}(t, x)} \right] = -\frac{\lambda_{\text{fr}}}{2D} \frac{q_{\text{NG}}(t, x) |q_{\text{NG}}(t, x)|}{\rho_{\text{NG}}(t, x)}, \quad (1.1b)$$

<sup>1</sup>University of Mannheim, Department of Mathematics, 68131 Mannheim, Germany (ulke@uni-mannheim.de, goettlich@uni-mannheim.de)

<sup>2</sup>Friedrich-Alexander University Erlangen-Nürnberg, Department of Mathematics, 91058 Erlangen, Germany (michi.schuster@fau.de)

the transport of a two-gas-mixture can be modeled by mass conservation (1.1a) for each gas and momentum balance (1.1b) for the mixing, cf. [6, 22, 28], i.e.,

$$\partial_t \rho_{\text{NG}}(t, x) + \partial_x q_{\text{NG}}(t, x) = 0, \quad (1.2a)$$

$$\partial_t \rho_{\text{H}_2}(t, x) + \partial_x q_{\text{H}_2}(t, x) = 0, \quad (1.2b)$$

$$\partial_t q(t, x) + \partial_x \left[ p(\rho_{\text{NG}}(t, x), \rho_{\text{H}_2}(t, x)) + \frac{q^2(t, x)}{\rho(t, x)} \right] = -\frac{\lambda_{\text{fr}}}{2D} \frac{q(t, x)|q(t, x)|}{\rho(t, x)}. \quad (1.2c)$$

The time-space domain is  $(t, x) \in [0, t_{\text{final}}] \times [0, L]$ . Furthermore,  $\rho_{\text{NG}}, \rho_{\text{H}_2}$  describe the densities and  $q_{\text{NG}}, q_{\text{H}_2}$  the flow of natural gas and hydrogen,  $\rho = \rho_{\text{NG}} + \rho_{\text{H}_2}$  and  $q = q_{\text{NG}} + q_{\text{H}_2}$  are the density and the flow of the mixture, respectively. Further,  $D > 0$  is the pipe diameter and  $\lambda_{\text{fr}}$  the pipe friction coefficient. The pressure-density relation of the gas is described by an appropriate state equation or pressure law. For pure natural gas, the pressure is commonly expressed as

$$p_{\text{NG}}(\rho_{\text{NG}}) = \frac{RT}{M_{\text{NG}}} Z(p_{\text{NG}}) \rho_{\text{NG}},$$

where  $R$  denotes the universal gas constant,  $M_{\text{NG}}$  the molar mass of natural gas,  $T$  the constant gas temperature, and  $Z(p_{\text{NG}})$  the compressibility factor.

For natural gas transport, the modeling of the compressibility factor is well established in the literature. Common choices include a constant approximation corresponding to the *ideal gas law*, cf. [10, 15, 32], linear approximations such as those proposed by the *American Gas Association*, cf. [18, 30], and quadratic models based on *Papay's formula*, cf. [30, 36]. These approximations are widely used in both stationary and transient gas network models and have proven to yield reliable results for pure natural gas flow. However, for gas mixtures, well established choices are still missing. While the molar mass of a mixture is typically defined as a convex combination of molar masses of the individual constituents, no universally accepted model exists for the corresponding compressibility factor. Several approaches have been proposed in the literature, primarily in the context of numerical simulations. For instance, [5, 35] approximates the compressibility factor of the mixture by a convex combination of constant compressibility factors, whereas [7] employs a convex combination of linear compressibility models. Further, [4] adopts a different strategy by combining critical temperatures and molar masses in order to apply a quadratic compressibility factor.

Although these approaches are all inspired by well-established compressibility models for pure natural gas, their extension to hydrogen-natural gas mixtures is not unique. Different modeling choices lead to distinct pressure-density relations and, consequently, to noticeably different steady states, even under identical boundary conditions, as shown in Figure 1. For the constant compressibility factor [5, 35], we apply

$$Z(p_{\text{NG}}) = Z(p_{\text{H}_2}) = 1, \quad (1.3)$$

and for the linear model [7, 30], we use

$$Z(p) = 1 + (\eta \alpha_{\text{H}_2} + (1 - \eta) \alpha_{\text{NG}}) p \quad \text{with} \quad \alpha_X = \frac{0.257}{p_{c,X}} - \frac{0.5333}{p_{c,X}} \frac{T_{c,X}}{T}, \quad (1.4)$$

where  $X \in \{\text{H}_2, \text{NG}\}$ ,  $p$  is the pressure of the mixture and  $\eta$  is the percentage of hydrogen in the mixture. Further,  $T$  is the gas temperature and  $p_{c,X}, T_{c,X}$  are the critical pressure and

temperature of the gases. The quadratic model [30, 4] is given by

$$Z(p) = 1 - 3.52 \exp\left(-2.26 \frac{T}{T_c}\right) \frac{p}{p_c} + 0.274 \exp\left(-1.878 \frac{T}{T_c}\right) \frac{p^2}{p_c^2}, \quad (1.5)$$

where  $p_c, T_c$  are the critical pressure and temperature of the mixture, computed by the convex combination of the critical pressure and temperature of the gases. The simulation results in Figure 1 demonstrate two effects: first, a clear difference between constant and non-constant compressibility models, with the non-constant models nearly coinciding for pure natural gas, and second, a growing discrepancy between the models as the hydrogen percentage increases. The lack of a canonical compressibility model for gas mixtures indicates that analytical results should not rely on a specific functional form of the compressibility factor.

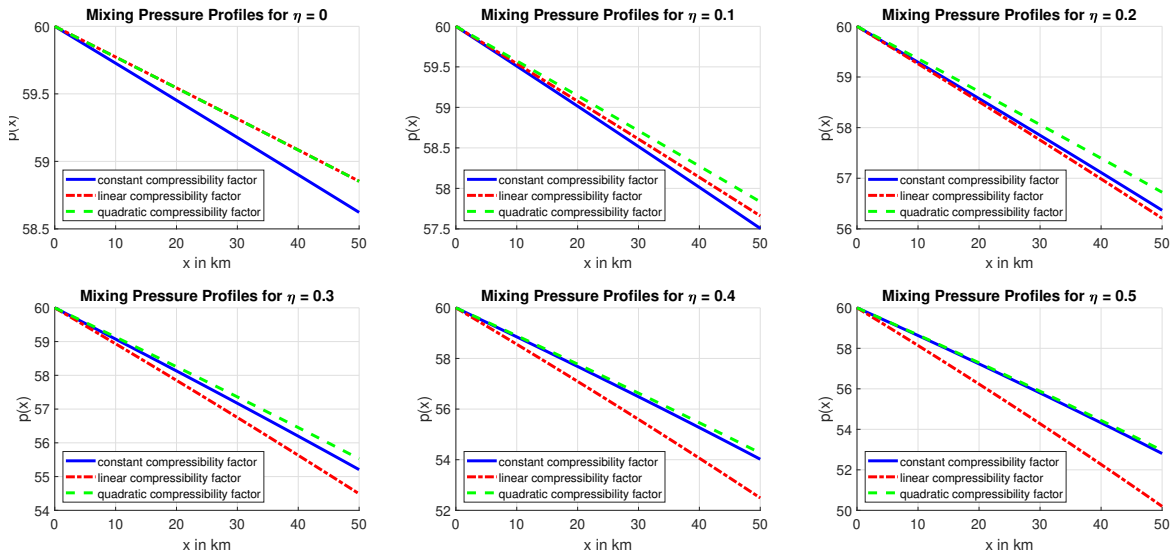


Figure 1: Simulation results for the compressibility factor models (1.3) - (1.5) on a single pipe with  $L = 50$  km,  $\lambda_{fr} = 0.05$  and  $D = 0.5$  m. The gas parameters are given by  $R = 8.3145 \text{ J}/(\text{mol K})^{-1}$ ,  $T = 283.15 \text{ K}$ ,  $p_{c,H_2} = 13.15 \text{ bar}$ ,  $p_{c,NG} = 46.01 \text{ bar}$ ,  $T_{c,H_2} = 33.19 \text{ K}$  and  $T_{c,NG} = 204.62 \text{ K}$ .

For the mixing model with a constant compressibility factor, the existence of steady states has been shown in [35] for pure transport networks. In contrast, the existence of steady-state solutions for the mixture model with non-constant compressibility factor and networks containing controllable elements such as compressor stations remains an open question. This gap motivates the present work, in which we establish the existence of steady states for a broad class of compressibility factors and extend the analysis to networks with compressor stations. The existence proof in [35] heavily utilizes that the pressure change along a path depends continuously on the boundary data, despite the discontinuous dependence of the composition on the flow direction. The key observation to establish the continuous dependence on the boundary data is that in the steady-state case, Equation (1.2) reduces to an ordinary differential equation (ODE) for the pressure profile. For ideal gas, this ODE admits a closed-form solution allowing us to analyze the influence of the discontinuities in composition on

the pressure change explicitly. For arbitrary compressibility factors, however, such a closed-form solution is unavailable in general. Thus, our key contribution is addressing the resulting technical difficulties.

This article is structured as follows: In Section 2, we introduce the gas flow model for mixtures on networks and derive an implicit solution of the ordinary differential equation arising from steady-state version of Equation (1.2) for arbitrary compressibility factors. Afterwards, we establish the existence of steady-state solutions for tree-shaped networks and networks with a single cycle in Section 3. Finally, in Section 4, we conclude with a numerical study showcasing the influence of different choices of the compressibility factor  $Z$  on the steady-state solution of the gas flow model for mixtures.

## 2 Modeling Gas Flow of Mixtures on Networks

Gas networks involve different elements, e.g., producers and consumers that deliver gas to and withdraw gas from the network, pipes to transport gas, and compressors to regulate pressure levels in the network. In the following, we introduce essential terminology and notation before we delve into the modeling of gas flow.

Let a directed, connected graph  $\mathcal{G} = (\mathcal{V}, \mathcal{E})$  with the set of nodes  $\mathcal{V}$ , which represent network junctions and serve as gas entry or exit points, and the set of edges  $\mathcal{E} \subseteq \mathcal{V} \times \mathcal{V}$  be given. Each edge  $e \in \mathcal{E}$  either represents a pipe of length  $L_e > 0$  or a compressor station with compressor ratio  $\gamma_e \geq 1$ , and we accordingly partition the edge set into the two disjoint subsets  $\mathcal{E}_{\text{pipe}} \subseteq \mathcal{E}$  and  $\mathcal{E}_{\text{comp}} \subseteq \mathcal{E}$  of pipes and compressors, respectively. For an edge  $e = (v, w) \in \mathcal{E}$ , let  $f(e) = v$  and  $h(e) = w$  denote the *start* of *foot node* and the *end* or *head node*, respectively. The set of nodes is given by the two disjoint sets  $\mathcal{V}_{<0}$ , representing the *supply nodes*, where gas is injected into the network, and  $\mathcal{V}_{\geq 0}$ , representing the *demand nodes*, where mass is conserved or gas is withdrawn from the network. For each node, we denote the set of *incoming* and *outgoing edges* by

$$\mathcal{E}_-(v) = \{e \in \mathcal{E} \mid e = (\bullet, v)\} \quad \text{and} \quad \mathcal{E}_+(v) = \{e \in \mathcal{E} \mid e = (v, \bullet)\},$$

respectively. The set  $\mathcal{E}(v) = \mathcal{E}_-(v) \cup \mathcal{E}_+(v)$  contains all edges incident to  $v$ . Further, we require the *node edge incidence matrix*  $A \in \mathbb{R}^{|\mathcal{V}| \times |\mathcal{E}|}$  with entries:

$$a(v, e) = \begin{cases} -1, & \text{if } v = f(e), \\ 1, & \text{if } v = h(e), \\ 0, & \text{otherwise.} \end{cases} \quad (2.1)$$

In order to describe gas flow on a network, we split the dynamic into three: the flow along pipes, the flow across nodes, and the operation of compressors.

### 2.1 Gas Flow through Pipes

The gas flow in pipeline networks is governed by the *isothermal Euler equations* (1.1), a system of hyperbolic partial differential equations (PDEs). Isothermality implies constant gas temperature over space and time. Since we are interested in the flow of mixtures consisting of hydrogen and natural gas, we consider a framework allowing for mixtures composed of two arbitrary constituents  $i \in \{1, 2\}$ . We assume perfect mixing, i.e., both constituents have the

same velocity and temperature. Within this framework, we can model the flow of hydrogen and natural gas by setting hydrogen as constituent  $i = 1$  and natural gas as constituent  $i = 2$ , cf. (1.2). Let  $\eta_e$  be the mass fraction of the first constituent (i.e., hydrogen) in the mixture on edge  $e \in \mathcal{E}$ . Thus, (1.2) is equivalent to the system:

$$\partial_t \rho_e + \partial_x q_e = 0, \quad (2.2a)$$

$$\partial_t (\eta_e \rho_e) + \partial_x (\eta_e q_e) = 0, \quad (2.2b)$$

$$\partial_t q_e + \partial_x \left[ p_e + \frac{q_e^2}{\rho_e} \right] = - \frac{\lambda_{\text{fr}}}{2D_e} \frac{q_e |q_e|}{\rho_e}, \quad (2.2c)$$

where  $\rho_e$  denotes the gas density,  $q_e$  the mass flow,  $p_e$  the pressure of the gas mixture. The constants  $D_e$  and  $\lambda_{\text{fr}}$  denote the diameter and friction factor of the pipe, respectively. The pressure and density are connected by the state equation

$$p_e(\rho_e) = \frac{RT}{M} Z(p_e) \rho_e,$$

where  $R$  is the universal gas constant,  $T$  the temperature,  $M$  the molar mass, and  $Z(p_e) > 0$  the compressibility factor of the gas. When analyzing the flow of gas mixtures, it is important to note that variations in the composition result in varying gas properties, including the molar mass and compressibility factor. However, since the gas mixture is always composed of the same fixed constituents, we can express the gas properties of a mixture based on the composition and properties of its constituents, i.e., the molar mass  $M$  and the compressibility factor  $Z$  also depend on the gas composition. For the remainder of this section, we omit the subscript  $e$  to improve the readability.

We determine the molar mass of a gas mixture based on the molar masses  $M_i$  of its constituents, along with the *molar fraction*  $\eta_{\text{mol}}$  of the first constituent, cf. [4, 5]. The molar mass  $M$  of the mixture is then given by

$$M = \eta_{\text{mol}} M_1 + (1 - \eta_{\text{mol}}) M_2. \quad (2.3)$$

We can also express the molar mass  $M$  in terms of mass fraction  $\eta$  by using the relation:

$$\eta_{\text{mol}} = \frac{n_1}{n_1 + n_2} \quad \text{with} \quad n_1 = \frac{\eta}{M_1}, \quad n_2 = \frac{1 - \eta}{M_2}, \quad (2.4)$$

where  $n_i$  is the number of moles of constituent  $i$  in the mixture. We substitute the molar fraction  $\eta_{\text{mol}}$  in Equation (2.3) by using the relation (2.4), which yields:

$$M = M(\eta) = \frac{M_1 M_2}{\eta M_2 + (1 - \eta) M_1} \quad \Leftrightarrow \quad \frac{1}{M(\eta)} = \frac{\eta}{M_1} + \frac{(1 - \eta)}{M_2}. \quad (2.5)$$

Next, we model dependence of the compressibility factor  $Z$  on the gas composition, which we express using the mass fraction since the relation (2.4) allows us to convert the mass fraction  $\eta$  into the molar fraction  $\eta_{\text{mol}}$  and vice versa:

$$\eta_{\text{mol}} = \frac{\eta M_2}{\eta M_2 + (1 - \eta) M_1} \quad \text{and} \quad \eta = \frac{\eta_{\text{mol}} M_1}{\eta_{\text{mol}} M_1 + (1 - \eta_{\text{mol}}) M_2}. \quad (2.6)$$

As there exist multiple approaches to model the compressibility factor, cf. [26], we adopt a general approach and treat the compressibility factor as a function of the pressure  $p$  and the mass fraction  $\eta$ , satisfying the following assumptions:

**Assumption 1.** The compressibility factor  $Z(\eta, p)$  is integrable and differentiable with respect to  $p$  for every mass fraction  $\eta \in [0, 1]$  and pressure  $p \in [0, \infty)$ .

**Assumption 2.** The compressibility factor  $Z(\eta, p)$  is differentiable with respect to  $\eta$  for every mass fraction  $\eta \in [0, 1]$  and pressure  $p \in [0, \infty)$ .

Finally, we obtain the pressure law for gas mixtures linking the pressure  $p$ , the density  $\rho$  and the composition of the gas, which is encoded through the mass fraction  $\eta$ :

$$p(\rho) = \frac{RT}{M(\eta)} Z(\eta, p) \rho = \left[ \frac{RT}{M_1} \eta + \frac{RT}{M_2} (1 - \eta) \right] Z(\eta, p) \rho. \quad (2.7)$$

Since we aim to analyze the steady state gas flow, the temporal derivatives in the Euler equations (2.2) vanish. As a result, the first two equations in the isothermal Euler equations imply that the mass flow  $q$  and the mass fraction  $\eta$  are constant along the pipe, reducing the PDE system to an ordinary differential equation (ODE):

$$\partial_x \left[ p(x) + \frac{q^2}{\rho(x)} \right] = -\frac{\lambda_{\text{fr}}}{2D} \frac{q|q|}{\rho(x)} \quad \text{for } x \in [0, L]. \quad (2.8)$$

In the following, we solve this ODE to obtain the pressure profile  $p(x)$  along the pipe and split the derivation of the pressure profile into two steps:

- (i) We eliminate the density  $\rho$  from the ODE using the pressure law (2.7), which yields an ODE depending only on the variables  $q$ ,  $\eta$ , and  $p$ .
- (ii) We solve the ODE from (i) for the pressure  $p$  using separation of variables.

We begin by transforming the ODE (2.8) into an ODE independent of the density  $\rho$ . First, we consider the right side of the equation and invoke the pressure law (2.7):

$$-\frac{\lambda_{\text{fr}}}{2D} \frac{q|q|}{\rho} = -\frac{\lambda_{\text{fr}}}{2D} \frac{RT}{M(\eta)} \frac{Z(\eta, p)}{p} q|q|.$$

Next, we consider the left side of the equation, where we additionally invoke the chain rule, which results in:

$$\begin{aligned} \partial_x \left[ p + \frac{q^2}{\rho} \right] &= \partial_x \left[ p + \frac{RT}{M(\eta)} q^2 \frac{Z(\eta, p)}{p} \right] = \partial_x p + \frac{RT}{M(\eta)} q^2 \partial_p \left[ \frac{Z(\eta, p)}{p} \right] \partial_x p, \\ &= \left[ 1 + \frac{RT}{M(\eta)} q^2 \left( \frac{\partial_p Z(\eta, p)}{p} - \frac{Z(\eta, p)}{p^2} \right) \right] \partial_x p. \end{aligned}$$

Recall that the mass flow  $q$  and the mass fraction  $\eta$  are constant along the pipe. Combining

both, we obtain the following formulation for the pressure loss ODE (2.8):

$$\begin{aligned} & \left[ 1 + \frac{RT}{M(\eta)} q^2 \left( \frac{\partial_p Z(\eta, p)}{p} - \frac{Z(\eta, p)}{p^2} \right) \right] \partial_x p = -\frac{\lambda_{\text{fr}}}{2D} \frac{RT}{M(\eta)} \frac{Z(\eta, p)}{p} q |q|, \\ \Leftrightarrow & \underbrace{\left[ \frac{p}{Z(\eta, p)} + \frac{RT}{M(\eta)} q^2 \left( \frac{\partial_p Z(\eta, p)}{Z(\eta, p)} - \frac{1}{p} \right) \right]}_{=F'(\eta, q, p)} \partial_x p = -\frac{\lambda_{\text{fr}}}{2D} \frac{RT}{M(\eta)} q |q|. \end{aligned} \quad (2.9)$$

The next step is to solve the ODE using separation of variables. Since we have already manipulated the equation into a form suitable for direct integration with respect to  $x$ , we only need an anti-derivative of  $F'$ , which – up to the integration constant – reads:

$$F(\eta, q, p) = \int \frac{p}{Z(\eta, p)} dp + \frac{RT q^2}{M(\eta)} [\ln(|Z(\eta, p)|) - \ln(|p|)]. \quad (2.10)$$

Thus, integrating the ODE (2.9) with respect to  $x$  yields:

$$F(\eta, q, p(x)) = F(\eta, q, p(0)) - \frac{\lambda_{\text{fr}}}{2D} \frac{RT}{M(\eta)} q |q| x \quad \text{for } x \in [0, L]. \quad (2.11)$$

*Remark 2.1.* As there are a variety of approaches to model the compressibility factor  $Z$  of a gas (mixture), we provide a brief overview. We also determine the integral  $\int \frac{p}{Z(\eta, p)} dp$  for these examples, since it does not have a closed form expression for general  $Z$ .

- For a constant approximation of the compressibility factor  $Z(\eta, p) = k \in \mathbb{R}$  (cf., (1.3) and [5, 32, 15, 35]), we obtain:

$$\int \frac{p}{Z(\eta, p)} dp = \frac{1}{2k} p^2.$$

- For a linear approximation of the compressibility factor  $Z(\eta, p) = 1 + \alpha p$ , where  $\alpha$  is given by the convex combination of the gas specific constants  $\alpha_{\text{H}_2}$  and  $\alpha_{\text{NG}}$  (cf., (1.4) and [7, 30, 18, 17]), we obtain

$$\int \frac{p}{Z(\eta, p)} dp = \frac{p}{\alpha_1 \eta + \alpha_2 (1 - \eta)} - \frac{\ln(|Z(\eta, p)|)}{[\alpha_1 \eta + \alpha_2 (1 - \eta)]^2}.$$

- For a quadratic approximation of the compressibility factor (1.5) (cf., *Papay's formula*, see [4, 30, 36]), where  $T_c(\eta_{\text{mol}})$  and  $p_c(\eta_{\text{mol}})$  are critical temperature and pressure, obtained by a convex combination of the critical temperature and pressure of the components, the integral in (2.10) reads

$$\begin{aligned} \int \frac{p}{Z(\eta_{\text{mol}}, p)} dp &= \frac{\ln(|Z(\eta_{\text{mol}}, p)|)}{2b} - \frac{a}{b\sqrt{4b - a^2}} \arctan \left( \frac{2bx + a}{\sqrt{4b - a^2}} \right), \\ \text{where } a &= \frac{1}{p_c(\eta_{\text{mol}})} \exp \left( -\frac{T}{T_c(\eta_{\text{mol}})} \right), \quad b = \frac{1}{p_c(\eta_{\text{mol}})^2} \exp \left( -\frac{T}{T_c(\eta_{\text{mol}})} \right). \end{aligned}$$

We obtain the pressure profile  $p(x)$  from Equation (2.11) if the function  $F$  is invertible with respect to  $p$ . In the regularity analysis of  $F$ , we make extensive use of one key physical

property: gas networks operate under subsonic conditions, i.e., the gas velocity  $v$  is smaller than the sound speed  $\sigma$  in the gas, to ensure system safety and prevent structural damage [9, 14]. For subsonic flow, the Mach number  $\text{Ma} := v/\sigma$  satisfies  $\text{Ma} < 1$ , which leads to:

$$\text{Ma}^2 = \left(\frac{v}{\sigma}\right)^2 < 1 \Leftrightarrow \frac{RT}{M(\eta)} \frac{q^2}{p^2} [Z(\eta, p) - p \cdot \partial_p Z(\eta, p)] < 1, \quad (2.12)$$

where we used the pressure law (2.7), the relation  $q = v\rho$ , and the following expression for the sound speed:

$$\left(\frac{1}{\sigma}\right)^2 = \partial_p \rho = \partial_p \left[ \frac{M(\eta)}{RT} \frac{p}{Z(\eta, p)} \right] = \frac{M(\eta)}{RT} \frac{Z(\eta, p) - p \cdot \partial_p Z(\eta, p)}{Z(\eta, p)^2}.$$

Since we are in a subsonic regime, we define the domain of subsonic flow by multiplying Equation (2.12) with  $p^2$ :

$$D_{\text{subsonic}} := \left\{ (\eta, q, p) \in [0, 1] \times \mathbb{R} \times [0, \infty) \mid p^2 - \frac{RT}{M(\eta)} q^2 [Z(\eta, p) - p \cdot \partial_p Z(\eta, p)] > 0 \right\}.$$

We proceed by proving that the function  $F$  is strictly monotonically increasing with respect to  $p$  for subsonic flows.

**Lemma 2.2.** *Let  $D_F \subseteq \{(\eta, q, p) \in [0, 1] \times \mathbb{R} \times [0, \infty) \mid Z(\eta, p) > 0\} \cap D_{\text{subsonic}}$  and define*

$$F: D_F \rightarrow \mathbb{R} \quad \text{with} \quad F(\eta, q, p) = \int \frac{p}{Z(\eta, p)} dp + \frac{RT q^2}{M(\eta)} \ln \left( \left| \frac{Z(\eta, p)}{p} \right| \right).$$

*Then, the function  $F$  is differentiable and strictly monotonically increasing on  $D_F$ .*

*Proof.* The differentiability of  $F$  follows directly from its derivation since it arises as an anti-derivative when solving the differential equation (2.8). The derivative of  $F$  with respect to  $p$  is given by

$$\partial_p F(\eta, q, p) = \frac{p}{Z(\eta, p)} + \frac{RT}{M(\eta)} q^2 \left[ \frac{\partial_p Z(\eta, p)}{Z(\eta, p)} - \frac{1}{p} \right] = \frac{p^2 - \frac{RT}{M(\eta)} q^2 [Z(\eta, p) - p \cdot \partial_p Z(\eta, p)]}{p \cdot Z(\eta, p)}.$$

Since we are in a subsonic regime and due to the choice of  $D_F$ , we have

$$p^2 - \frac{RT}{M(\eta)} q^2 [\partial_p Z(\eta, p) - Z(\eta, p)] > 0 \quad \text{and} \quad Z(\eta, p) \geq 0.$$

Thus,  $\partial_p F(\eta, q, p) > 0$  holds, which means that  $F$  is strictly monotonically increasing.  $\square$

Together with the Implicit Function Theorem, Theorem 2.2 implies that  $F$  is locally bijective with respect to the pressure  $p$ .

**Corollary 2.3.** *The function  $F: D_F \rightarrow \mathbb{R}$  defined in Theorem 2.2 is locally bijective with respect to the pressure  $p$ . Further, the corresponding inverse  $(\eta, q, y) \mapsto g(\eta, q, y)$  is continuous and satisfies:*

$$F(\eta, q, p) = y \Leftrightarrow p = g(\eta, q, y).$$

*Proof.* The claim follows immediately from the Implicit Function Theorem applied to the function  $f(\eta, q, p, y) = F(\eta, q, p) - y$  since  $\partial_p f(\eta, q, p, y) = \partial_p F(\eta, q, p)$  and according to Theorem 2.2, we have  $\partial_p F(\eta, q, p) \neq 0$ .  $\square$

In summary, we recover the pressure profile  $p(x)$  from Equation (2.11) by applying the inverse  $p \mapsto g(\eta, q, p)$ . Then, the pressure profile  $p(x)$  on each pipe  $e$  has the following form:

**Lemma 2.4.** *Let  $q \in \mathbb{R}$  be the gas flow and  $\eta \in [0, 1]$  the mass fraction. Then the solution to the pressure ODE (2.8) reads*

$$p(x) = g\left(\eta, q, F(\eta, q, p(0)) - \frac{\lambda_{\text{fr}}}{2D} \frac{RT}{M(\eta)} q |q| x\right).$$

*Remark 2.5.* For friction-dominated pressure loss, the nonlinear term  $\partial_x (q^2/\rho)$  can be neglected, resulting in the semi-linear isothermal Euler equations (see, e.g., [9, 24]). Solving the pressure loss for steady states of the semi-linear equations is analogous to the derivation above, but the function  $F$  is replaced by

$$F_{\text{semi}}(\eta, q, p) = \int \frac{p}{Z(\eta, p)} \, dp.$$

The domain  $D_F$  in Theorem 2.2 satisfies  $Z(\eta, p) > 0$ . Thus, the function  $F_{\text{semi}}$  is also strictly monotonically increasing with respect to  $p$  and the results of Theorem 2.2 and Theorem 2.4 also apply for the semi-linear isothermal Euler equations.

## 2.2 Gas Flow across Junctions

Gas flow across nodes is governed by *coupling conditions*, see, e.g., [3, 9, 24]. For gas mixtures, these consists of the following:

- (i) The mass of the mixture as well as the individual constituents is conserved.
- (ii) The gas mixes perfectly and instantaneously, i.e., one obtains a homogeneous mixture without time delay.
- (iii) The pressure is continuous across a node.

Mass conservation and pressure continuity also appear in single gas flows, while the perfect mixing condition is unique for the flow of gas mixtures.

**Mass Balance.** Let  $b_v \in \mathbb{R}$  be the *load* of node  $v \in \mathcal{V}$ , i.e., the amount of gas entering or leaving the network. We have

$$\begin{aligned} b_v < 0 &\Leftrightarrow v \in \mathcal{V}_{<0}, \text{ which means } v \text{ is a supply node,} \\ b_v \geq 0 &\Leftrightarrow v \in \mathcal{V}_{\geq 0}, \text{ which means } v \text{ is a demand node.} \end{aligned}$$

Then, the mass balance across node  $v \in \mathcal{V}$  refers to the fact that the sum of all incoming flows and all outgoing flows is equal to the load. Using the incidence matrix  $A \in \mathbb{R}^{|\mathcal{V}| \times |\mathcal{E}|}$ , cf. Equation (2.1), the mass balance for the network is given by the linear system

$$\sum_{e \in \mathcal{E}} a(v, e) q_e = b_v \quad \text{for all } v \in \mathcal{V} \Leftrightarrow A\mathbf{q} = \mathbf{b},$$

where  $\mathbf{b} \in \mathbb{R}^{|\mathcal{V}|}$  is the load vector with entries  $b_v$ , and  $\mathbf{q} \in \mathbb{R}^{|\mathcal{E}|}$  the flow vector with entries  $q_e$ .

**Perfect Mixing and Mass Balance of the Constituents.** Perfect and instantaneous mixing means that incoming gas immediately forms a homogeneous mixture at the node before flowing into the outgoing pipes. As a result, the composition of the outgoing gas is identical across all pipes, which automatically ensures the mass balance of the individual constituents. Since the flow direction and the edge orientation can differ, it is unclear a priori which pipes carry incoming and which carry outgoing flow. However, a pipe  $e$  supplies gas to the node if  $a(v, e)q_e \geq 0$ , and it transports gas away from the node if  $a(v, e)q_e < 0$ . For each supply node  $v \in \mathcal{V}_{<0}$ , let  $\zeta_v \in [0, 1]$  be mass fraction of the first constituent of the supply node. Then, the nodal mass fraction  $\eta_v$  becomes

$$\eta_v = \frac{\sum_{e \in \mathcal{E}(v)} \eta_e (a(v, e)q_e)^+ + \zeta_v b_v^-}{\sum_{e \in \mathcal{E}(v)} (a(v, e)q_e)^+ + b_v^-},$$

where for a scalar  $\alpha \in \mathbb{R}$ , we define  $\alpha^+ = \max\{\alpha, 0\}$  and  $\alpha^- = \max\{-\alpha, 0\}$ . Additionally, we have the following relation between the nodal mass fraction  $\eta_v$  and the mass fraction  $\eta_e$  along a pipe:

$$\eta_e = \begin{cases} \eta_{f(e)}, & \text{if } q_e \geq 0, \\ \eta_{h(e)}, & \text{if } q_e < 0, \end{cases} \quad (2.13)$$

which encodes that the mass fraction along a pipe is always given by the upstream nodal composition.

**Pressure Continuity.** Pressure continuity ensures that all pipes connected to a node  $v$  have the same pressure at the shared endpoint. To enforce this, we introduce the nodal pressure  $p_v$ , leading to the condition:

$$p_e(x_e) = p_v \quad \text{for all } e \in \mathcal{E}(v) \quad \text{where} \quad x_e = \begin{cases} 0, & e \in \mathcal{E}_-(v), \\ L_e, & e \in \mathcal{E}_+(v). \end{cases}$$

Together with Equation (2.11), which describes the pressure loss between along a pipe  $e$ , we obtain the pressure loss between two connected, adjacent nodes:

$$F(\eta_e, q_e, p_{h(e)}) - F(\eta_e, q_e, p_{f(e)}) = -\frac{\lambda_{\text{fr}}}{2D} \frac{RT}{M(\eta_e)} L_e q_e |q_e|.$$

We recall that the specific expression for  $F$  depends on the compressibility factor  $Z$ , cf. Equation (2.10).

### 2.3 Operation of Compressors

Compressors play a key role in the operation of gas networks as they can increase the pressure locally. Since pipeline networks need to operate within a certain pressure range to ensure safe operation, and since the transport of gas alone causes a drop in pressure due to friction, compressors are needed to counteract the pressure loss and to maintain a safe pressure level.

Each compressor  $e \in \mathcal{E}_{\text{comp}}$  is equipped with a so-called *boosting* or *compressor ratio*  $\gamma_e \geq 1$  and we assume that the compressor ratio is independent of the gas composition, cf. [19, 22].

The operation of a compressor is governed by the pressure boost equation:

$$p_{h(e)} = \gamma_e p_{f(e)} \quad \text{where } e = (f(e), h(e)). \quad (2.14)$$

Compressor stations are designed to increase the pressure only in one direction, gas flow in the opposite direction is not possible, cf. [9, 24]. Thus, we make the following assumption:

**Assumption 3.** For every edge  $e \in \mathcal{E}_{\text{comp}}$ , the gas flows from node  $f(e)$  to node  $h(e)$ , i.e., we have  $q_e \geq 0$  for all  $e \in \mathcal{E}_{\text{comp}}$ .

Thus, the composition of the gas in the compressor is given by the upstream composition  $\eta_e = \eta_{f(e)}$ . Furthermore, we prohibit compressors from forming pathological structures such as cycles or running parallel to other edges to prevent circular gas flow in a cycle.

## 2.4 Full Gas Flow Model

Summarizing, the steady state gas flow model for mixtures includes the pressure loss along pipes together with the pressure continuity across nodes, the compressor property, the mass balance and the mixing condition. This is given by

$$F(\eta_e, q_e, p_{h(e)}) - F(\eta_e, q_e, p_{f(e)}) = -\frac{\lambda_{\text{fr}}}{2D} \frac{RT}{M(\eta_e)} L_e q_e |q_e| \quad \text{for all } e \in \mathcal{E}_{\text{pipe}}, \quad (2.15a)$$

$$p_{h(e)} = \gamma_e p_{f(e)} \quad \text{for all } e \in \mathcal{E}_{\text{comp}}, \quad (2.15b)$$

$$\sum_{e \in \mathcal{E}_+(v)} q_e - \sum_{e \in \mathcal{E}_-(v)} q_e = b_v \quad \text{for all } v \in \mathcal{V}, \quad (2.15c)$$

$$\eta_v = \frac{\sum_{e \in \mathcal{E}(v)} \eta_e (a(v, e) q_e)^+ + \zeta_v b_v^-}{\sum_{e \in \mathcal{E}(v)} (a(v, e) q_e)^+ + b_v^-} \quad \text{for all } v \in \mathcal{V}. \quad (2.15d)$$

In comparison to the setting in [35], the gas flow model (2.15) also accommodates compressor stations and non-constant compressibility factors. The major difference is Equation (2.15a) as the function  $F$  is no longer explicitly available for arbitrary compressibility factors. For ideal gas, where  $Z = 1$  holds, we have  $F(\eta, q, p) = \frac{1}{2}p^2$ , which recovers [35, Equation 2.15].

## 3 Existence of Steady-State Solutions

We show the existence of solutions to the model (2.15) for networks with up to one cycle by extending the approach presented in [18] for the gas flow of one constituent using the quasi-linear model and assuming real gas, and in [35] for gas mixtures made up of two constituents using the semi-linear model and assuming ideal gas. Compared to the setting in [18, 35], the novelty lies in generalizing the existence result to arbitrary compressibility factors  $Z$  instead of assuming a constant or linear compressibility factor. This generalization comes with a major difficulty: for non-constant compressibility factors, the pressure change along a path connecting two nodes lacks a closed-form expression in general. We will indicate in detail where and how this lack of an explicit representation introduces additional challenges in the proof compared to ideal gas.

### 3.1 Tree-Shaped Networks

The proof for tree-shaped networks is straightforward since the model equations decouple and we can solve the model equations subsequently: first for the flow  $q_e$ , then for the mass fraction  $\eta_v$ , and finally for the pressure  $p_v$ .

**Theorem 3.1** (Existence of Solution for Trees). *Let  $\mathcal{G} = (\mathcal{V}, \mathcal{E})$  be a tree-shaped network and let  $v^* \in \mathcal{V}$  be an arbitrary yet fixed node. Further, provide*

- (i) *the load  $b_v$  for all  $v \in \mathcal{V}$  satisfying  $\sum_{v \in \mathcal{V}} b_v = 0$ ,*
- (ii) *the supply composition  $\zeta_v \in [0, 1]$  for all  $v \in \mathcal{V}$  with  $b_v \leq 0$ ,*
- (iii) *the compressor ratio  $\gamma_e \geq 1$  for all  $e \in \mathcal{E}_{\text{comp}}$ , and*
- (iv) *the nodal pressure  $p_v$  for  $v = v^*$ .*

*Further, assume that the compressibility factor  $Z$  satisfies Assumption 1 and 2 and that the gas flow is subsonic. Then the steady-state mixture model admits a unique solution.*

*Proof.* The proof for the existence of unique solutions for tree-shaped networks is analogous to the proof of [35, Theorem 3.5]. However, we must additionally exploit that the function  $p \mapsto F(\eta, q, p)$  is locally bijective (Theorem 2.2) for fixed  $\eta \in [0, 1]$  when solving the pressure loss equation (2.15a).  $\square$

### 3.2 Networks With One Cycle

The presence of a cycle in a network makes proving the existence of steady states more intricate. In the following, we state the main theorem and provide the auxiliary results necessary to prove it.

**Theorem 3.2** (Existence of Solution for Networks with one Cycle). *Let  $\mathcal{G} = (\mathcal{V}, \mathcal{E})$  be a network with one cycle and let  $v^* \in \mathcal{V}$  be an arbitrary yet fixed node. Further, provide*

- (i) *the load  $b_v$  for all  $v \in \mathcal{V}$  satisfying  $\sum_{v \in \mathcal{V}} b_v = 0$ ,*
- (ii) *the supply composition  $\zeta_v \in [0, 1]$  for all  $v \in \mathcal{V}$  with  $b_v \leq 0$ ,*
- (iii) *the compressor ratios  $\gamma_e \geq 1$  for all  $e \in \mathcal{E}_{\text{comp}}$ , and*
- (iv) *the nodal pressure  $p_v$  for  $v = v^*$ .*

*Furthermore, assume that the compressibility factor  $Z$  satisfies Assumption 1 and 2 and that the gas flow is subsonic. Then the steady-state mixture model admits at least one solution.*

The idea to prove Theorem 3.2 is to cut an edge  $e^c$  of the cycle to obtain a tree-shaped network that has the same structure as the original, but without the cut edge  $e^c$  and with two additional nodes,  $v_\ell$  and  $v_r$  respectively, and two additional edges  $e_\ell = (f(e^c), v_\ell)$  and  $e_r = (v_r, h(e^c))$  generated by the cut. The resulting network is the so-called *cut network*  $\mathcal{G}^c$  of  $\mathcal{G}$  with respect to  $e^c$ , cf. [18, 37], and is defined by

$$\mathcal{G}^c = (\mathcal{V}^c, \mathcal{E}^c) \quad \text{with} \quad \mathcal{V}^c = \mathcal{V} \cup \{v_\ell, v_r\}, \quad \mathcal{E}^c = (\mathcal{E} \setminus \{e^c\}) \cup \{e_\ell, e_r\}.$$

The goal is to find solutions on the cut graph that are also solutions on the original graph. On the cut graph, such solutions have constant flow, mass fraction, and pressure through the cut. To extract these solutions, we must determine suitable boundary data – consisting of the load and supply composition – for the new nodes generated by the cut. Throughout this paper, we indicate variables that are associated with the cut graph using the superscript  $c$ .

As the relation  $b_{v_\ell}^c = -b_{v_r}^c$  enforces a constant flow through the cut automatically, we introduce the parameter  $\lambda$  and set  $b_{v_\ell}^c = \lambda$  and  $b_{v_r}^c = -\lambda$ . Additionally, we introduce the parameter  $\mu$  to model the supply composition either of node  $v_\ell$  or node  $v_r$  depending on the sign of  $\lambda$ . Then, the parameter-dependent boundary data on the cut network reads:

$$p_{v^*}^c = p^*, \quad b_v^c = \begin{cases} b_v, & v \in \mathcal{V}, \\ -\lambda, & v = v_r, \\ \lambda, & v = v_\ell, \end{cases} \quad \text{and} \quad \zeta_v^c = \begin{cases} \zeta_v, & v \in \mathcal{V}_{<0}, \\ \mu, & v = v_r \text{ and } \lambda \geq 0, \\ \mu, & v = v_\ell \text{ and } \lambda < 0. \end{cases} \quad (3.1)$$

The remaining two conditions – constant mass fraction and constant pressure through the cut – form a non-linear system that need to be solved for the parameters  $\lambda$  and  $\mu$ :

$$\mathcal{H}_\eta(\lambda, \mu) := \eta_{v_r}^c(\lambda, \mu) - \eta_{v_\ell}^c(\lambda, \mu) = 0 \quad (3.2a)$$

$$\mathcal{H}_p(\lambda, \mu) := p_{v_r}^c(\lambda, \mu) - p_{v_\ell}^c(\lambda, \mu) = 0. \quad (3.2b)$$

The equation  $\mathcal{H}_\eta = 0$  ensures constant mass fraction through the cut, while the equation  $\mathcal{H}_p = 0$  implies that the pressure is continuous though cut. Thus, showing that the non-linear system (3.2) admits at least one solution  $(\lambda^*, \mu^*) \in \mathbb{R} \times [0, 1]$  is equivalent to showing that there exists at least one solution to the gas flow model (2.15) for networks with one cycle, cf. [35, Lemma 3.8]. The proof to show the solvability of the non-linear system (3.2) follows the same fundamental argument developed in [35] for the setting of ideal gas together with the semi-linear pressure equation. The core idea is as follows:

- (i) Fix a cut edge  $e^c \in \mathcal{E}$ . Since the flow on the original network must be acyclic, we can restrict the admissible values for the solution  $\lambda^*$  to an interval  $I_{\text{sol}}$ .
- (ii) For each fixed  $\lambda \in I_{\text{sol}}$ , the function  $\mathcal{H}_\eta(\lambda, \mu)$  admits a unique root  $\mu_\eta(\lambda)$ .
- (iii) The function  $g(\lambda) = \mathcal{H}_p(\lambda, \mu_\eta(\lambda))$  satisfies the intermediate value theorem on the interval  $I_{\text{sol}}$ , i.e.,
  - (a) the function  $g$  is continuous on  $I_{\text{sol}}$ , and
  - (b) it attains opposite signs at the boundary values of  $I_{\text{sol}}$ .

Although the overall structure of the proof remains the same for our setting, the non-constant compressibility factor  $Z$  introduces significant technical difficulties. Figure 2 illustrates the structure of the proof and highlights the subtle yet significant argument that fails for arbitrary compressibility factors. The main difficulty arises in proving continuity. The idea is to show that the root curve  $\mu_\eta(\lambda)$  and the function  $\mathcal{H}_p(\lambda, \mu)$  are continuous in all arguments, since then  $g$  is continuous as composition of continuous functions. The composition on the cut graph is independent of the pressure, and hence of the compressibility factor  $Z$ , as the cut graph is tree-shaped. Therefore, the derivation of  $\mu_\eta$  is analogous to the case of ideal gas, cf. [35, Lemma 3.20]. For all  $\lambda \in \mathbb{R}$  such that gas does not flow from node  $v_\ell$  to node  $v_r$ ,

we obtain the following expression:

$$\mu_\eta(\lambda) = \begin{cases} \eta_{v_r}^c(\lambda), & \lambda < 0, \\ \eta_{v_\ell}^c(\lambda), & \lambda \geq 0. \end{cases}$$

Since the root curve  $\mu_\eta$  is given by the composition at either node  $v_\ell$  or node  $v_r$ , its continuity follows from the continuity of the composition. The continuity of the composition does not depend on the compressibility factor  $Z$ , whereas the continuity of  $\mathcal{H}_p$  does, cf. [35, Lemma 3.18, Lemma 3.21]. For ideal gas, where  $Z = 1$ , there exists an explicit expression of  $\mathcal{H}_p$  in terms of the flow and the composition. This explicit dependence allows us to derive the continuity of  $\mathcal{H}_p$  from the continuity of the flow and the composition, as provided by [35, Corollary 3.15, Lemma 3.16, Lemma 3.17]. However, there is one issue: the composition at the nodes generated by the cut is only right-sided continuous. Fortunately, the explicit dependence makes it possible to analyze the effect of the one-sided continuity at  $\lambda = 0$  on the continuity of  $\mathcal{H}_p$ , revealing that the discontinuity in fact vanishes.

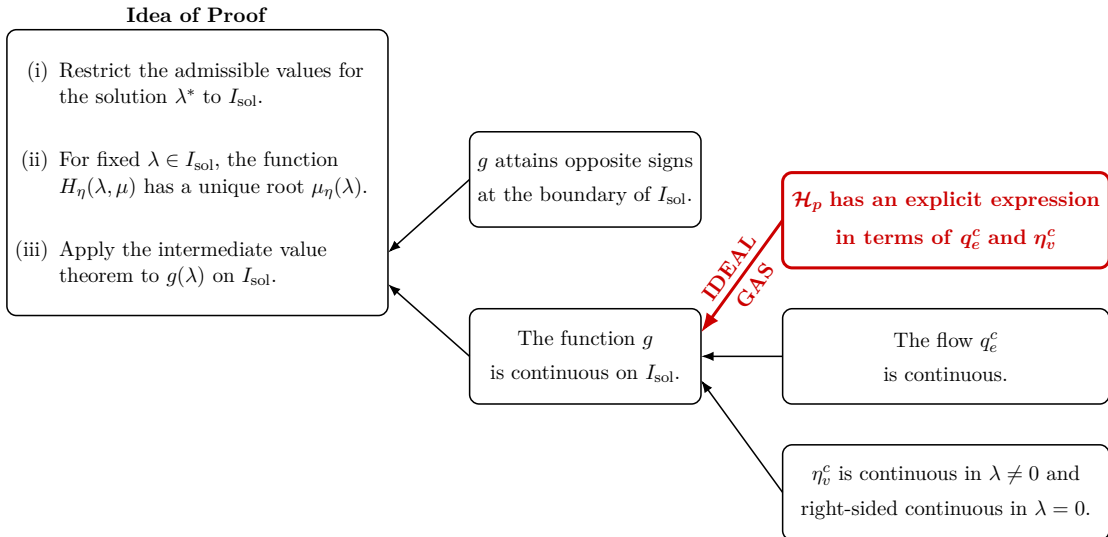


Figure 2: Key idea to prove existence of steady-states, and step at which the argumentation of [35, Lemma 3.13] for the ideal gas case fails for an arbitrary compressibility factor  $Z = Z(\eta, p)$  (highlighted in red).

For an arbitrary compressibility factor  $Z$ , the explicit dependence of  $\mathcal{H}_p$  on the flow and composition is unknown. Thus, it remains unclear how the discontinuity enters  $\mathcal{H}_p$  and it is not possible to verify that  $\mathcal{H}_p$  is also continuous at  $\lambda = 0$  immediately. To overcome this difficulty, we proceed with the following steps:

- We prove the continuity of  $\mathcal{H}_p$  for  $\lambda \neq 0$  and right-sided continuity at  $\lambda = 0$  using an induction argument.
- We show that a cut edge exists such that  $I_{\text{sol}} \subset [0, \infty)$ . This choice allows us to invoke the intermediate value theorem for  $g$  on  $I_{\text{sol}}$  immediately.

### 3.3 Continuity of Flow, Mass Fraction, and Pressure

Besides ensuring continuous pressure across the cut edge, the function  $\mathcal{H}_p$  also describes the pressure change along the path connecting the nodes  $v_r$  and  $v_\ell$ . We aim to establish the continuity of  $\mathcal{H}_p$  by an induction based argument utilizing Equation (2.15a). Therefore, we recall the continuity properties of the flow and composition. As the cut network is tree-shaped, the continuity result [35, Corollary 3.11] for ideal gas applies directly to our setting and provides the continuity of the flow. For the continuity of the mass fraction, we have:

**Lemma 3.3** (Continuity of the Mass Fraction). *Let  $\mathcal{G} = (\mathcal{V}, \mathcal{E})$  be a connected, directed graph with a cycle. Further, let  $e$  be an edge of the cycle and  $\mathcal{G}^c$  be the corresponding cut graph with boundary data as defined in Equation (3.1). Then the mass fraction  $\eta_v^c = \eta_v^c(\lambda, \mu)$  is*

- (i) continuous in  $\mu$  for all  $v \in \mathcal{V}^c$ ,
- (ii) continuous in  $\lambda \neq 0$  for all  $v \in \mathcal{V}^c$ ,
- (iii) continuous in  $\lambda = 0$  for all  $v \in \mathcal{V}^c \setminus \{v_\ell, v_r\}$ ,
- (iv) right-sided continuous in  $\lambda = 0$  for  $v \in \{v_\ell, v_r\}$ .

*Proof.* The continuity with respect to  $\mu$  follows directly from [35, Lemma 3.13], while the continuity with respect to  $\lambda$  in  $\lambda \neq 0$  for all  $v \in \mathcal{V}^c$  and in  $\lambda = 0$  for all  $v \notin \{v_\ell, v_r\}$  follows from [35, Lemma 3.12]. Furthermore, we can additionally exploit that the boundary data (3.1) is right-sided continuous in  $\lambda = 0$ , which yields together with [35, Lemma 3.12] the right-sided continuity in  $\lambda = 0$  for  $v \in \{v_\ell, v_r\}$ .  $\square$

For ideal gas, the continuity of the flow and the mass fraction immediately implies the continuity of  $\mathcal{H}_p$ , since in this case the pressure change along a path admits a closed-form representation that depends only on the flow and the mass fraction, cf. [35]. For real gases, the structure of the pressure law makes it in general impossible to express the pressure change along a path explicitly in terms of the flow and the composition. Nevertheless, we can still establish the continuity of  $\mathcal{H}_p$  with respect to  $\lambda$  and  $\mu$  with an induction based argument.

**Lemma 3.4** (Continuity of the Nodal Pressure). *Let  $\mathcal{G} = (\mathcal{V}, \mathcal{E})$  be a directed, connected graph,  $e^c$  be an edge of the cycle, and  $\mathcal{G}^c$  the cut graph corresponding to the cut edge  $e^c$ . Suppose boundary data according to Equation (3.1) is given. Then, for all  $v \in \mathcal{V}^c$ , the pressure  $p_v^c = p_v^c(\lambda, \mu)$  is*

- (i) continuous in  $\mu$ ,
- (ii) continuous in  $\lambda \neq 0$  and right-sided continuous in  $\lambda = 0$ .

*Proof.* We fix an arbitrary node  $v \in \mathcal{V}^c \setminus \{v^*\}$ . As the cut graph is tree-shaped, there exists only one path connecting  $v$  to  $v^*$ . We set the first node of the path to  $v_1 = v^*$  and traverse the path, successively labeling each node until we reach the end of the path, i.e., the node  $v_{n_v} = v$ . Then, the nodes of the path are given by  $v_i$  for  $i = 1, \dots, n_v$ . Further, two incident nodes  $v_i$  and  $v_{i+1}$  are connected by the edge  $e_i$ ; see Figure 3 for an illustration. To prove the continuity of  $p_v^c$ , we proceed with an induction over the position  $i$  of nodes along the path.

*Base case.* At position  $i = 1$ , we have the node  $v^*$ . Since the pressure at node  $v^*$  is given through boundary data, the pressure  $p_{v^*}^c$  is constant, and thus continuous in both  $\lambda$  and  $\mu$ .

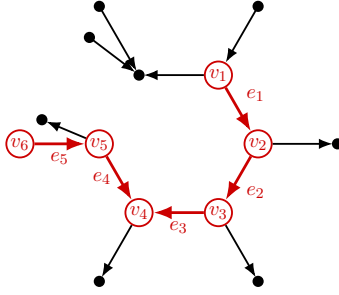


Figure 3: A cut network with the path connecting the node  $v_1 = v^*$  to the node  $v_6 = v$ . The path and the numbering are highlighted in red.

*Induction step.* Suppose the pressure  $p_{v_i}^c$  is continuous in  $\mu$  and in  $\lambda \neq 0$  as well as right-sided continuous in  $\lambda = 0$  for an arbitrary yet fixed  $i < n_v$ . The goal is to prove that – given the continuity of  $p_{v_i}^c$  – the pressure  $p_{v_{i+1}}^c$  is also continuous.

Therefore, we distinguish between two cases. The first case is that  $e_i = (v_i, v_{i+1})$  and the second one that  $e_i = (v_{i+1}, v_i)$ . We prove the first case. If the edge  $e_i$  is a pipe, we utilize Equation (2.15a) to express the pressure  $p_{v_{i+1}}^c$  in terms of the pressure  $p_{v_i}^c$ :

$$F(\eta_{e_i}^c, q_{e_i}^c, p_{v_{i+1}}^c) - F(\eta_{e_i}^c, q_{e_i}^c, p_{v_i}^c) = \underbrace{-\frac{\lambda_{\text{fr}}}{2D} \frac{RT}{M(\eta_{e_i}^c)} L_{e_i}^c q_{e_i}^c |q_{e_i}^c|}_{=S(\eta_{e_i}^c, q_{e_i}^c)}$$

with Theorem 2.3 this leads to:

$$\begin{aligned} F(\eta_{e_i}^c, q_{e_i}^c, p_{v_{i+1}}^c) &= F(\eta_{e_i}^c, q_{e_i}^c, p_{v_i}^c) + S(\eta_{e_i}^c, q_{e_i}^c) \\ \Leftrightarrow p_{v_{i+1}}^c &= g\left(\eta_{e_i}^c, q_{e_i}^c, F(\eta_{e_i}^c, q_{e_i}^c, p_{v_i}^c) + S(\eta_{e_i}^c, q_{e_i}^c)\right). \end{aligned}$$

Recall the dependencies  $\eta_{e_i}^c = \eta_{e_i}^c(\lambda, \mu)$ ,  $q_{e_i}^c = q_{e_i}^c(\lambda)$ , and  $p_{v_i}^c = p_{v_i}^c(\lambda, \mu)$ . From [35, Lemma 3.10] follows that  $q_{e_i}^c$  is continuous in  $\lambda$ . Theorem 3.3 together with Equation (2.13) implies that  $\eta_{e_i}^c$  is continuous in  $\mu$  and in  $\lambda \neq 0$  as well as right-sided continuous in  $\lambda = 0$ . Moreover, the function  $g$  is continuous in all of its components by Theorem 2.3, and  $S$  is continuous continuous by definition. Thus,  $p_{v_{i+1}}^c$  is continuous as a composition of continuous functions. If the edge  $e_i$  is a compressor, we have the relation  $p_{v_{i+1}}^c = \gamma_{e_i} p_{v_i}^c$ . However, in this case the continuity of  $p_{v_{i+1}}^c$  follows immediately since  $\gamma_{e_i}$  is a constant.

The case  $e_i = (v_{i+1}, v_i)$  is analogous and thus, as  $v = v_{n_v}$ , we obtain that  $p_v^c$  is continuous in  $\mu$  and in  $\lambda \neq 0$  as well as right-sided continuous in  $\lambda = 0$ .  $\square$

**Corollary 3.5.** *Let  $\mathcal{G} = (\mathcal{V}, \mathcal{E})$  be a directed, connected graph,  $e^c$  be an edge of the cycle, and  $\mathcal{G}^c$  the cut graph corresponding to the cut edge  $e^c$ . Suppose boundary data according to Equation (3.1) is given. Then the function  $\mathcal{H}_p(\lambda, \mu) = p_{v_r}^c(\lambda, \mu) - p_{v_\ell}^c(\lambda, \mu)$  is*

- (i) continuous in  $\mu$ ,
- (ii) continuous in  $\lambda \neq 0$  and right-sided continuous in  $\lambda = 0$ .

### 3.4 Existence of a Suitable Cut Edge

For the ideal gas case, we obtain the interval  $I_{\text{sol}}$  utilizing [35, Lemma 3.15]. The key observation here is that if  $\lambda$  is sufficiently small the gas flows from node  $v_r$  to node  $v_\ell$  in the cut graph, and if it is sufficiently large the gas flow in the opposite direction. On the original graph this translates into a circular gas flow. However, as the gas flow must be acyclic, we can now bound the admissible values for  $\lambda$  from below and above, which yields the interval  $I_{\text{sol}}$ . The boundary values of  $I_{\text{sol}}$  depend only on the flow  $q_e^c$  and loads  $b_v$  of the network as well as the network topology and the choice of the cut edge  $e^c$ . Hence, [35, Lemma 3.15] is independent from the pressure change equation and transfers to case of arbitrary compressibility factors  $Z$ .

As the interval  $I_{\text{sol}}$  depends on the cut edge, we aim to find a cut edge  $e^c$  such that  $I_{\text{sol}} \subset [0, \infty)$ . For ideal gases, the question of finding a *suitable* cut edge does not occur because in this case the function  $\mathcal{H}_p$  is continuous for all  $\lambda \in \mathbb{R}$ . To address this question for real gases, we take a closer look on the derivation of the interval  $I_{\text{sol}}$  and introduce necessary notation.

**Definition 3.6** (Sub-Graph of a Cycle). Let  $\mathcal{G} = (\mathcal{V}, \mathcal{E})$  be a directed, connected graph with a cycle. Then, the cycle forms a connected sub-graph  $\mathcal{G}_{\text{cycle}} = (\mathcal{V}_{\text{cycle}}, \mathcal{E}_{\text{cycle}})$  of the graph  $\mathcal{G}$  where  $\mathcal{V}_{\text{cycle}} \subseteq \mathcal{V}$  denotes the nodes, and  $\mathcal{E}_{\text{cycle}} \subseteq \mathcal{E}$  the edges of the cycle. Further,  $n_{\text{cycle}} = |\mathcal{V}_{\text{cycle}}|$  denotes the number of nodes in the cycle.

**Definition 3.7** (Sub-Graph of a Cut Cycle). Let  $\mathcal{G} = (\mathcal{V}, \mathcal{E})$  be a directed, connected graph with a cycle and let  $e^c \in \mathcal{E}_{\text{cycle}}$  be an edge in the cycle. By cutting the edge  $e^c$ , we obtain the cut graph  $\mathcal{G}_{\text{cycle}}^c = (\mathcal{V}_{\text{cycle}}^c, \mathcal{E}_{\text{cycle}}^c)$  of the cycle, where

$$\mathcal{V}_{\text{cycle}}^c = \mathcal{V}_{\text{cycle}} \cup \{v_\ell, v_r\}, \quad \mathcal{E}_{\text{cycle}}^c = \mathcal{E}_{\text{cycle}} \setminus \{e^c\} \cup \{e_\ell, e_r\},$$

The cut graph  $\mathcal{G}_{\text{cycle}}^c$  is tree-shaped and only consists of a single path connecting the two new nodes  $v_\ell$  and  $v_r$ . It also forms a sub-graph of the cut graph  $\mathcal{G}^c$  of  $\mathcal{G}$ .

The flow on the edges of the cut cycle is linear in  $\lambda$  and independent of  $\mu$ , cf. [35, Lemma 3.10], which implies that each flow  $q_e^c$  has a unique root  $\beta_e$  with respect to  $\lambda$  for all  $e \in \mathcal{E}_{\text{cycle}}^c$ . Together with [35, Lemma 3.15], we can identify suitable boundary values  $\lambda^\pm$  for the interval  $I_{\text{sol}} = [\lambda^-, \lambda^+]$  and summarize the finding in the following lemma.

**Lemma 3.8.** *Let  $\mathcal{G} = (\mathcal{V}, \mathcal{E})$  be a directed, connected graph with one cycle and let  $e^c \in \mathcal{E}_{\text{cycle}}$  be the cut edge. Further, denote the root of the flow  $q_e^c$  with respect to  $\lambda$  by  $\beta_e$  for  $e \in \mathcal{E}_{\text{cycle}}^c$ , cf. [35, Lemma 3.10], and set:*

$$\lambda^- = \min_{e \in \mathcal{E}_{\text{cycle}}^c} \beta_e \quad \text{and} \quad \lambda^+ = \max_{e \in \mathcal{E}_{\text{cycle}}^c} \beta_e,$$

*Then a solution  $(\lambda^*, \mu^*)$  to the non-linear system (3.2) must satisfy  $\lambda^* \in [\lambda^-, \lambda^+]$ . Furthermore, the values  $\lambda^\pm$  satisfy the following inequalities:*

$$\mathcal{H}_p(\lambda^-, \mu) \leq 0 \quad \text{and} \quad \mathcal{H}_p(\lambda^+, \mu) \geq 0 \quad \text{for all } \mu \in [0, 1].$$

*Proof.* The proof is analogous to [35, Lemma 3.15] for the case of an ideal gas, because the flow on the cut graph is independent of the pressure law since the cut graph is tree-shaped. The proof exploits the fact that pressure decreases in the flow direction, i.e., gas flow must be

acyclic unless there is a compressor in a cycle, but this is prohibited by assumption. For real gas, pressure also decreases in the flow direction, because with Equation (2.15a), we have:

$$F(\eta_e, q_e, p_{h(e)}) - F(\eta_e, q_e, p_{f(e)}) = \underbrace{-\frac{\lambda_{\text{fr}}}{2D} \frac{RT}{M(\eta_e)} L_e |q_e| q_e}_{<0} \\ \Rightarrow \text{sign}(F(\eta_e, q_e, p_{h(e)}) - F(\eta_e, q_e, p_{f(e)})) = -\text{sign}(q_e).$$

When the gas flows from node  $f(e)$  to node  $h(e)$ , we have  $q_e \geq 0$  and thus,

$$F(\eta_e, q_e, p_{h(e)}) \leq F(\eta_e, q_e, p_{f(e)}).$$

Due to the monotonicity of  $F$  with respect to the pressure  $p$ , cf. Theorem 2.2, we get  $p_{h(e)} \leq p_{f(e)}$ . The case when gas flows in the opposite direction, i.e., from node  $h(e)$  to node  $f(e)$ , follows analogously and results in  $p_{h(e)} \geq p_{f(e)}$  as here we have  $q_e \leq 0$ .  $\square$

The values  $\beta_e$  depend on the choice of cut edge  $e^c$ , and consequently so does the interval  $I_{\text{sol}}$ . Therefore, the question whether there exists a cut edge  $e^c$  such that  $I_{\text{sol}} \subset [0, \infty)$ , is equivalent to finding a cut edge  $e^c$  such that  $\beta_e \geq 0$  for all  $e \in \mathcal{E}_{\text{cycle}}^c$ .

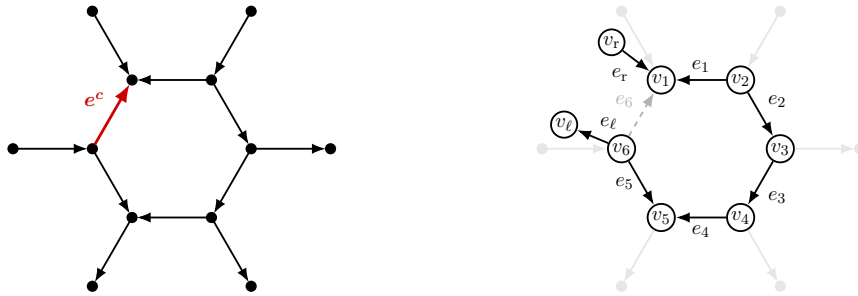


Figure 4: A gas network with cut edge  $e^c$  and  $n_{\text{cycle}} = 6$  (left), and the corresponding cut graph with nodes and edges of the former cycle being numbered (right).

In the following, it is crucial to understand the derivation and computation of the values  $\beta_e$ . Therefore, we fix a cut edge  $e^c$  and number the nodes and edges of the cycle. For the nodes, we set  $v_1 = h(e^c)$  and traverse through the cycle, successively labeling each subsequent node until we reach the end of the cycle, where we set  $v_{n_{\text{cycle}}} = f(e^c)$ ; see Figure 4 for an illustration. For the edges, we follow a similar pattern: each edge  $e_i$  connects the nodes  $v_i$  and  $v_{i+1}$  for  $i = 1, \dots, n_{\text{cycle}} - 1$  with the exception of the edge  $e_{n_{\text{cycle}}} = e^c$ , which connects the nodes  $v_{n_{\text{cycle}}}$  and  $v_1$  closing the cycle.

With this notation at hand, we can express the flow  $q_e^c$  on an edge of the former cycle as a linear function with respect to  $\lambda$ , which introduces the values  $\beta_e$ :

**Lemma 3.9** (see [35, Lemma 3.10] and [18, Theorem 1]). *Let  $\mathcal{G} = (\mathcal{E}, \mathcal{V})$  be a network with one cycle and let  $e^c \in \mathcal{E}_{\text{cycle}}$  be the cut edge. Then, the flow on the edges  $e \in \mathcal{E}_{\text{cycle}}^c$  of the former cycle is linear in  $\lambda$ . Adapting the numbering of nodes and edges illustrated in Figure 4,*

the flow  $q_{e_i}^c$  on these edges for  $i \in \{1, \dots, n_{\text{cycle}} - 1\}$  reads:

$$a^c(v_i, e_i)q_{e_i}^c(\lambda) = \beta_{e_i} - \lambda \quad \text{where} \quad \beta_{e_i} = \sum_{j=1}^i b_{v_j}^{\mathcal{P}}, \quad (3.3)$$

$$b_v^{\mathcal{P}} = b_v - \sum_{e \in \mathcal{E}(v) \setminus \mathcal{E}_{\text{cycle}}^c} a^c(v, e)q_e^c \quad \text{for } v \in \mathcal{V}_{\text{cycle}},$$

where  $a^c(v, e)$  refers to the entries of the incident matrix  $A^c$  of the cut graph  $\mathcal{G}^c$ . Alternatively, the flow  $q_{e_i}^c$  can be written as

$$a^c(v_{i+1}, e_i)q_{e_i}^c(\lambda) = \tilde{\beta}_{e_i} + \lambda \quad \text{where} \quad \tilde{\beta}_{e_i} = \sum_{j=1}^{n_{\text{cycle}}-i} b_{v_{n_{\text{cycle}}-j+1}}^{\mathcal{P}}. \quad (3.4)$$

Further, the new edges  $e_r$  and  $e_\ell$  generated by the cut satisfy:

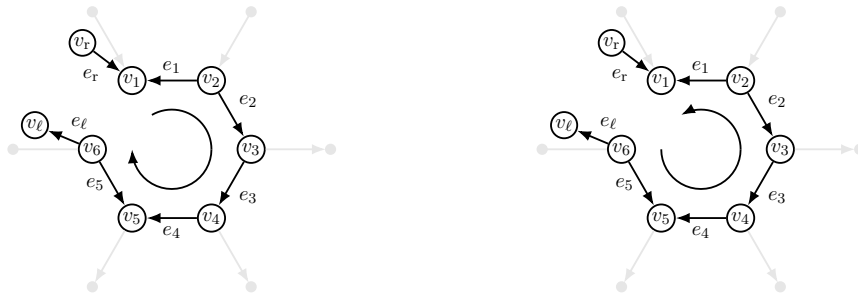
$$q_{e_r}^c(\lambda) = \lambda \quad \text{and} \quad q_{e_\ell}^c(\lambda) = \lambda \quad \Rightarrow \quad \beta_{e_r} = \beta_{e_\ell} = 0 \quad \text{and} \quad \tilde{\beta}_{e_r} = \tilde{\beta}_{e_\ell} = 0.$$

*Remark 3.10.* In Equation (3.3), we traverse the nodes of the former cycle from  $v_r = v_0$  to  $v_\ell = v_{n_{\text{cycle}}+1}$ , whereas in Equation (3.4), we traverse the nodes in the reversed direction. The values  $\beta_{e_i}$  are the partial sums of the modified loads  $b_v^{\mathcal{P}}$  starting at  $v_1$ , proceeding forward along the path connecting the nodes  $v_r$  and  $v_\ell$ . In contrast, the values  $\tilde{\beta}_{e_i}$  are the reversed partial sums, traversing the nodes in the opposite direction, see Figure 5 for an illustration.

In summary, Theorem 3.9 allows us to express  $\lambda^\pm$  in terms of the values  $\beta_{e_i}$  using the notation illustrated in Figure 4, i.e.,

$$\lambda^- = \min M_\beta, \quad \lambda^+ = \max M_\beta, \quad \text{where} \quad M_\beta = \{\beta_{e_i} \mid 1 \leq i \leq n_{\text{cycle}} - 1\} \cup \{0\}.$$

It also shows that a cut edge such that  $0 \notin I_{\text{sol}}$  cannot exist. As the values  $\beta_{e_r}$  and  $\beta_{e_\ell}$  are independent of the cut edge, we always have  $0 \in I_{\text{sol}}$ . Thus, finding a cut edge such that  $I_{\text{sol}} \subset [0, \infty)$  implies that 0 must lie on the left boundary of  $I_{\text{sol}}$ .



$(v_6, v_1)$  as the cut edge for the network in Figure 6. Then we can still apply Theorem 3.9 while keeping the original numbering. In this case, the values  $\beta_{e_i}$  associated with the cut edge  $e_4$  are given by the partial sums starting at  $v_5$ . Once the summation reaches the node  $v_6$ , it continues with the node  $v_1$ :

$$\begin{aligned}\beta_{e_5} &= b_{v_5}^P, & \beta_{e_6} &= b_{v_5}^P + b_{v_6}^P, \\ \beta_{e_1} &= b_{v_5}^P + b_{v_6}^P + b_{v_1}^P, & \beta_{e_2} &= b_{v_5}^P + b_{v_6}^P + b_{v_1}^P + b_{v_2}^P, \\ \beta_{e_3} &= b_{v_5}^P + b_{v_6}^P + b_{v_1}^P + b_{v_2}^P + b_{v_3}^P,\end{aligned}$$

To formalize this procedure, we introduce the concept of partial sums with wrapping.



Figure 6: A gas network with cut edge  $e^c$  and the corresponding numbering (left), and the cut graph with cut edge  $\tilde{e}^c = e_4$  while keeping the previous numbering (right).

**Definition 3.11** (Partial Sum with Wrapping). Let  $(y_j)_{j=1}^n \subseteq \mathbb{R}$  be a finite sequence of real numbers and let  $k \in \{1, \dots, n\}$  be a fixed index. Then the partial sum  $T_i(k)$  with wrapping starting at the element  $y_k$  is defined by

$$T_i(k) = \begin{cases} \sum_{j=k}^n y_j + \sum_{j=1}^{(k+i-1)-n} y_j, & k+i-1 > n, \\ \sum_{j=k}^{k+i-1} y_j, & k+i-1 \leq n. \end{cases}$$

Thus, the question whether there exists a cut edge  $e^c$  such that  $\beta_e \geq 0$  becomes: Can we determine an index  $k^* \in \{1, \dots, n_{\text{cycle}}\}$  for the sequence  $(b_{v_j}^P)_{j=1}^{n_{\text{cycle}}}$  such that all partial sums with wrapping  $T_i(k^*)$  are non-negative? The answer gives the following result:

**Lemma 3.12** (Existence of Non-Negative Partial Sums with Wrapping). *Let  $(y_j)_{j=1}^n$  be a finite sequence which satisfies  $\sum_{j=1}^n y_j = 0$ . Then there exists an index  $k^*$  such that*

$$T_i(k^*) \geq 0 \quad \text{for all } i \in \{1, \dots, n\}.$$

*Proof.* We compute the partial sums  $S_k$  of the sequence  $(y_j)_{j=1}^n$  and determine their minimum. In particular, we have:

$$m := \arg \min_{i \in \{1, \dots, n\}} S_i \quad \text{where} \quad S_i := \sum_{j=1}^i y_j \quad \Rightarrow \quad S_i \geq S_m \quad \text{for all } i \in \{1, \dots, n\}.$$

In case the minimal partial sum is non-unique, we choose  $m$  as the maximum among all minimizing indices  $\tilde{m}$ . Then, the partial sums  $T_i(m+1)$  starting at the element  $x_{m+1}$  satisfy  $T_i(m+1) \geq 0$  for all  $i \in \{1, \dots, n\}$ . In order to prove this, we distinguish two cases:

(i) Let  $m + i > n$  and recall that  $S_n = \sum_{j=1}^n y_j = 0$  holds. Then we have

$$T_i(m+1) = \sum_{j=m+1}^n y_j + \sum_{j=1}^{m+i-n} y_j = S_n - S_m + S_{m+i-n} = S_{m+i-n} - S_m \geq 0,$$

(ii) Let  $m + i \leq n$ . Then we have

$$T_i(m+1) = \sum_{j=m+1}^{m+i} y_j = S_{m+i} - S_m \geq 0,$$

Thus, setting  $k^* = m + 1$  proves the claim.  $\square$

*Remark 3.13.* If an index  $k^*$  satisfies  $T_i(k^*) \geq 0$ , then summing in the reversed order and starting at the predecessor  $x_{k^*-1}$  yields non-positive partial sums.

Next, we transfer Theorem 3.12 to our application – the existence non-negative  $\beta_e$ .

**Lemma 3.14.** *Let  $\mathcal{G} = (\mathcal{V}, \mathcal{E})$  be a network with one cycle. Then, there exists a cut edge  $e^c \in \mathcal{E}_{\text{cycle}}$  such that the corresponding values  $\beta_e$ , as defined in Theorem 3.9, satisfy*

$$\beta_e \geq 0 \quad \text{for all } e \in \mathcal{E}_{\text{cycle}},$$

up to a possible change the orientation of an edge  $e \in \mathcal{E}_{\text{cycle}}$  in the cycle.

*Proof.* Fix an arbitrary edge  $\tilde{e} \in \mathcal{E}_{\text{cycle}}$  of the cycle – not necessarily the cut edge – and number the nodes and edges of the cycle as described in Figure 4. Since the values  $\beta_{e_i}$  are the partial sums (with wrapping) of the modified loads  $b_v^P$ , cf. Theorem 3.9, and since the modified loads sum up to zero, we can apply Theorem 3.12 to the sequence  $(b_{v_j}^P)_{j=1}^{n_{\text{cycle}}}$ . Thus, we obtain an index  $k^*$  such that the corresponding partial sums with wrapping  $T_i(k^*)$  are all non-negative, i.e.,

$$T_i(k^*) \geq 0 \quad \text{for all } i = 1, \dots, n_{\text{cycle}}.$$

Now, we have to distinguish between the case where  $e_{k^*} = (v_{k^*-1}, v_{k^*})$  and the case where  $e_{k^*} = (v_{k^*}, v_{k^*-1})$ . In the first case, we choose  $e_{k^*} = (v_{k^*-1}, v_{k^*})$  as the cut edge and apply Theorem 3.9, which yields

$$\beta_{e_i} = T_i(k^*) \geq 0 \quad \text{for all } i = 1, \dots, n_{\text{cycle}}.$$

In the second case, we have  $e_{k^*} = (v_{k^*}, v_{k^*-1})$ . However, in this case setting the cut edge to  $e^c = e_{k^*}$  does not lead to the desired results because the computation of  $\beta_e$  relies on traversing the nodes of the cut cycle from  $v_r$  to  $v_\ell$ . But cutting the edge  $e_{k^*}$  and computing the partial sums  $T_i(k^*)$  corresponds to traversing the nodes of the cut cycle from  $v_\ell$  to  $v_r$ , which means that

$$T_i(k^*) = \tilde{\beta}_{e_i},$$

where  $\tilde{\beta}_e$  is defined in Equation (3.4); see also Figure 5. Together with Theorem 3.13 this implies that  $\beta_e \leq 0$ . We resolve this problem by replacing the network  $\mathcal{G}$  with the network  $\tilde{\mathcal{G}} = (\mathcal{V}, \tilde{\mathcal{E}})$  where the edge  $e_{k^*}$  is flipped, i.e.,  $\tilde{e}_{k^*} = (v_{k^*-1}, v_{k^*}) \in \tilde{\mathcal{E}}$ . Applying the above analysis to the network  $\tilde{\mathcal{G}}$ , we arrive at the same index  $k^*$  but since we flipped the edge orientation, we fall into in the first case instead.  $\square$

*Remark 3.15.* When the second case in the proof applies, we have to continue the analysis of finding a solution to the gas flow model (2.15) with the modified network  $\tilde{\mathcal{G}}$ . Once we found a solution for the network  $\tilde{\mathcal{G}}$ , we recover a solution for the original network  $\mathcal{G}$  by reversing the sign of the flow on the flipped edge.

With Theorem 3.14 at hand, we can select a cut edge such that  $\beta_e \geq 0$  for all  $e \in \mathcal{E}_{\text{cycle}}$ , which allows us to prove that the non-linear system (3.2) has at least one solution also for real gases with an arbitrary compressibility factor  $Z$ .

**Lemma 3.16.** *Let  $\mathcal{G} = (\mathcal{V}, \mathcal{E})$  be a connected, directed graph with one cycle. Further, let  $e^c$  be a suitable edge belonging to the cycle and let  $\mathcal{G}^c$  be the corresponding cut graph with the boundary data given in Equation (3.1). Then, the following non-linear system, also compare Equation (3.2), has at least one solution:*

$$\mathcal{H}_\eta(\lambda, \mu) = 0 \quad \text{and} \quad \mathcal{H}_p(\lambda, \mu) = 0.$$

*Proof.* First, we determine a suitable cut edge  $e^c$  with Theorem 3.14 and we set the interval  $I_{\text{sol}} = [\lambda^-, \lambda^+]$  according to Theorem 3.8. Then the function  $g(\lambda) = \mathcal{H}_p(\lambda, \mu_\eta(\lambda))$  is continuous on  $I_{\text{sol}}$  as the root curve  $\mu_\eta$  is continuous on  $I_{\text{sol}}$  with Theorem 3.3 and the function  $\mathcal{H}_p$  is continuous on  $I_{\text{sol}} \times [0, 1]$  with Theorem 3.5. Moreover, by applying Theorem 3.8, we obtain that  $g$  attains opposite sign on the boundary of  $I_{\text{sol}}$ . Finally, the intermediate value theorem yields that the function  $g$  has at least one root  $\lambda^*$  in  $I_{\text{sol}}$ . Hence, due to the definition of the curve  $\mu_\eta$  and the function  $g$ , we obtain that  $(\lambda^*, \mu_\eta(\lambda^*))$  solves the non-linear system (3.2).  $\square$

Finally, we are able to proof the Theorem 3.2, thereby extending the result that the gas flow model (2.15) has at least one solution also for arbitrary compressibility factors.

*Proof of Theorem 3.2.* Choose an edge  $e^c$  belonging to the cycle of the graph  $\mathcal{G}$ , which satisfies Theorem 3.14, and set it as the cut edge. Further, let  $\mathcal{G}^c = (\mathcal{V}^c, \mathcal{E}^c)$  be the corresponding cut graph with parameter-dependent boundary data as defined in Equation (3.1). Then, the non-linear system (3.2) has at least one solution, see Theorem 3.16. Hence, by [35, Lemma 3.8], the gas flow model (2.15) admits at least one solution.  $\square$

## 4 A Numerical Example on GasLib-11

To illustrate the practical implications of the theoretical results derived before, we present a numerical example demonstrating the influence of different compressibility factor models on the resulting steady states. In particular, we show that the choice of compressibility model affects not only the pressure profiles (cf., Figure 1) but also the resulting hydrogen concentrations in the network. The simulations are carried out on the GasLib-11<sup>1</sup> benchmark network (see Figure 7), which consists of 11 nodes, 8 edges, two compressor stations, and one valve that can be interpreted as a friction-free pipe. The network contains a single cycle, making it well suited to highlight the effects of model choice in a setting consistent with the analytical framework developed in this work.

In this example, natural gas consists of 90% methane, 6% ethane and 4% propane. For the readers' convenience we assume that pipe friction coefficient, pipe diameter and pipe length

---

<sup>1</sup>Network data can be found on <https://gaslib.zib.de/>

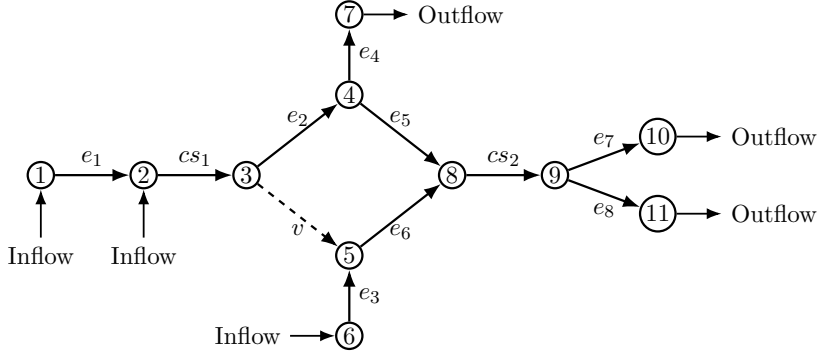


Figure 7: GasLib-11 with eleven nodes, eight pipes, two compressor stations and one valve.

are equal for every pipe  $e_i$ . The network and gas parameters are listed in Table 1. The gas pressure at the inflow nodes and the gas demand at the outflow nodes is given by

$$\begin{pmatrix} p_1 & p_2 & p_6 \end{pmatrix}^\top = \begin{pmatrix} 60 & 58 & 63 \end{pmatrix}^\top \text{bar}, \quad \begin{pmatrix} b_7 & b_{10} & b_{11} \end{pmatrix}^\top = \begin{pmatrix} 120 & 80 & 90 \end{pmatrix}^\top \frac{\text{kg}}{\text{m}^2 \text{s}}.$$

Parameter	Variable	Value	Unit
pipe friction coefficient	$\lambda_{\text{fr}}$	0.05	
pipe diameter	$D$	0.5	m
pipe length	$L$	10	km
universal gas constant	$R$	8.3145	$\text{J}/(\text{mol K})^{-1}$
gas temperature	$T$	283.15	K
critical pressure of hydrogen	$p_{c,\text{H}_2}$	13.15	bar
critical pressure of natural gas	$p_{c,\text{NG}}$	46.01	bar
critical temperature of hydrogen	$T_{c,\text{H}_2}$	33.19	K
critical temperature of natural gas	$T_{c,\text{NG}}$	204.62	K

Table 1: Parameters and coefficients for the example on GasLib-11

The first compressor station is switched off, i.e.,  $\gamma_{cs_1} = 1$ , and for the second compressor station we have  $\gamma_{cs_2} = 1.2$ . Further, we assume that at node 1, pure natural gas is injected, at node 2, pure hydrogen is injected and at node 6, a composition of 25% hydrogen and 75% natural gas is injected. A solution of the model (2.15) exists for the approximations (1.3), (1.4) and (1.5) due to Theorem 3.2. The solution is shown in Figure 8, it was computed using the *AMPL* software with the *ipopt* solver (see [13]), while the pictures were created in *MATLAB® 2023b*.

The difference in the pressure profiles is clearly visible at the outflow nodes. While the constant compressibility model (1.3) leads to 40.85 bar, 48.54 bar and 47.54 bar at the outflow nodes, the linear compressibility model (1.4) leads to lower pressures of 38.64 bar, 46.08 bar and 44.88 bar, and the quadratic compressibility model (1.5) leads to higher pressures given by 44.41 bar, 50.73 bar and 49.87 bar. This observation is consistent with the simulation results shown in Figure 1: the longer the transport distance - and, correspondingly, the further downstream in the network - the more pronounced the differences in the pressure

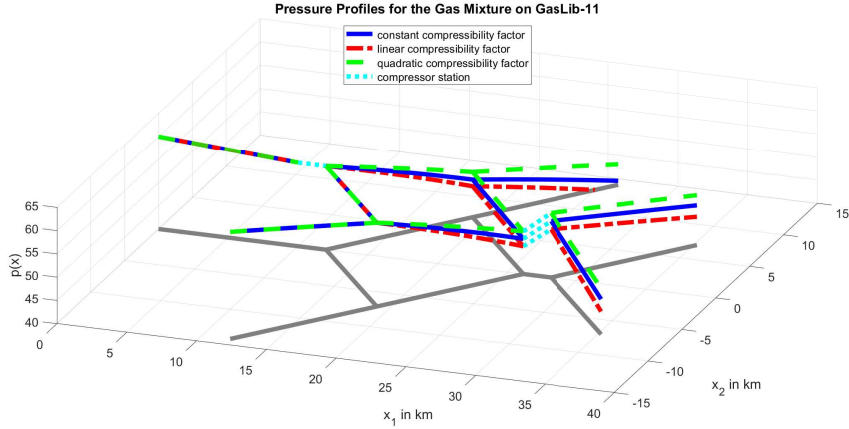


Figure 8: Simulation results for the mixing model on the GasLib–11

profiles between the respective compressibility models become. However, in contrast to the simulation on a single pipe in Figure 1, the network structure implies that the inflows, and thus the gas compositions in the pipes, also depend on the compressibility model. These results are given in Table 2, where  $q_{\text{in}}$  is the inflow at the nodes 1, 2 and 6, and  $\eta_{\text{out}}$  is the composition at the nodes 7, 10 and 11.

	constant approximation	linear approximation	quadratic approximation
$q_{\text{in}}$	$\begin{pmatrix} 134.36 & 59.09 & 96.55 \end{pmatrix} \frac{\text{kg}}{\text{m}^2\text{s}}$	$\begin{pmatrix} 147.01 & 60.30 & 82.69 \end{pmatrix} \frac{\text{kg}}{\text{m}^2\text{s}}$	$\begin{pmatrix} 146.98 & 45.49 & 97.53 \end{pmatrix} \frac{\text{kg}}{\text{m}^2\text{s}}$
$\eta_{\text{out}}$	$\begin{pmatrix} 0.4429 & 0.4159 & 0.4159 \end{pmatrix}$	$\begin{pmatrix} 0.4204 & 0.3926 & 0.3926 \end{pmatrix}$	$\begin{pmatrix} 0.4348 & 0.3876 & 0.3876 \end{pmatrix}$

Table 2: Gas flow at the entry nodes and gas composition at the exit nodes

## 5 Conclusion

Different compressibility factor models for hydrogen-natural gas mixtures used in the literature, lead to noticeably different steady states, even with identical boundary conditions. This highlights that analytical results for the flow of gas mixtures should not rely on a specific functional form of the compressibility factor, but rather cover a general class of models.

In this work, we established the existence of steady states for the transport of gas mixtures in pipeline networks for a broad class of non-constant, composition-dependent compressibility factors. The analysis applies to tree-shaped networks, as well as networks containing a cycle and also includes compressor stations. In contrast to ideal gas, for real gases the pressure can only be represented implicitly. Furthermore, the mixture model exhibits an additional difficulty: both pressure and composition depend on the flow direction, leading to discontinuities in the modeling. The existence proof is based on an implicit formulation of the steady-state pressure along pipes, combined with a continuity analysis. For networks with a cycle, the argument relies on cutting the cycle to obtain a tree-shaped network, solving the resulting problem with parameter-dependent boundary data, and exploiting the topological

structure of the network to control the dependence of the pressure on flow and composition. This approach allows to overcome the lack of an explicit representation for the pressure and the discontinuous dependence induced by considering gas mixtures.

The results presented here provide a rigorous analytical foundation for further investigations of hydrogen-natural gas transport in pipeline networks. In particular, they open the door to optimal control problems for compressor operation and network management. Although such problems are well established for single-gas transport networks (see, e.g., [1, 2, 15, 20, 21, 27, 31]), only numerical studies exist so far for gas mixture transport (see, e.g., [7, 23, 29]), and a comprehensive analytical treatment is still missing. The existence results derived in this paper constitute a first step towards a systematic analysis of optimal control and optimization problems for gas mixture networks with realistic real-gas effects.

**Acknowledgements** Two of the authors were supported by the German Research Foundation (DFG) in the Collaborative Research Center CRC/Transregio 154, Mathematical Modelling, Simulation and Optimization using the Example of Gas Networks, Project C03, Projektnumer 239904186 (Michael Schuster) as well as under the grant GO 1920/12-1, Projektnumer 526006304 (Simone Göttlich).

## References

- [1] L. Baker, S. Kazi, R. Platte, and A. Zlotnik. “Optimal Control of Transient Flows in Pipeline Networks with Heterogeneous Mixtures of Hydrogen and Natural Gas”. In: *2023 American Control Conference (ACC)*. 2023, pp. 1221–1228.
- [2] M. Banda and M. Herty. “Towards a Space Mapping Approach to Dynamic Compressor Optimization of Gas Networks”. In: *Optim. Control Appl. Meth.* 32 (2011), pp. 253–269.
- [3] M. K. Banda, M. Herty, and A. Klar. “Coupling conditions for gas networks governed by the isothermal Euler equations”. In: *Netw. Heterog. Media* 1.2 (2006), pp. 295–314. DOI: 10.3934/nhm.2006.1.295.
- [4] A. Bermúdez and M. Shabani. “Numerical simulation of gas composition tracking in a gas transportation network”. In: *Energy* 247 (2022). DOI: 10.1016/j.energy.2022.123459.
- [5] P. Börner, M. Pfetsch, and S. Ulbrich. “Modeling and optimization of gas mixtures on networks”. In: *Operations Research Proceedings 2024*. Ed. by L. Glomb. Springer Nature Switzerland, 2025.
- [6] D. Bothe and W. Dreyer. “Continuum thermodynamics of chemically reacting fluid mixtures”. In: *Acta Mech.* 226 (2015), pp. 1757–1805.
- [7] Y. Brodskyi, V. Gyrya, and A. Zlotnik. “Simulation of gas mixture dynamics in a pipeline network using explicit staggered-grid discretization”. In: *Appl. Math. Model.* 137 (2025). DOI: 10.1016/j.apm.2024.115717.
- [8] Bundesregierung. *Energy from climate-friendly gas*. 2024. URL: <https://www.bundesregierung.de/breg-de/klimaschutz-energie-und-klimapolitik/energie-und-klima/energie-und-klima/energy-from-climate-friendly-gas-1303327>
- [9] P. Domschke, B. Hiller, J. Lang, and C. Tischendorf. *Modellierung von Gasnetzwerken: Eine Übersicht*. Tech. rep. 2717. TU Darmstadt, 2017. URL: <http://www3.mathematik.tu-darmstadt.de/.../2717.pdf>
- [10] P. Domschke, O. Kolb, and J. Lang. “Fast and reliable transient simulation and continuous optimization of large-scale gas networks”. In: *Math. Methods Oper. Res.* 95 (2022), pp. 475–501.

- [11] European Commission. *A hydrogen strategy for a climate-neutral Europe*. 2020. URL: [https://energy.ec.europa.eu/system/files/2020-07/hydrogen\\_strategy\\_0.pdf](https://energy.ec.europa.eu/system/files/2020-07/hydrogen_strategy_0.pdf).
- [12] European Hydrogen Backbone. *Five hydrogen supply corridors for Europe in 2030 - Executive Summary*. 2022. URL: <https://ehb.eu/files/downloads/EHB-Supply-corridors-presentat>
- [13] R. Fourer, D. Gay, and B. Kernighan. *AMPL A Modeling Language for Mathematical Programming*. Second. DUXBURY, 2002.
- [14] M. Gugat, F. Hante, M. Hirsch-Dick, and G. Leugering. “Stationary states in gas networks”. In: *Netw. Heterog. Media* 10.2 (2015), pp. 295–320. DOI: [10.3934/nhm.2015.10.295](https://doi.org/10.3934/nhm.2015.10.295).
- [15] M. Gugat, M. Schuster, and J. Sokolowski. “The location problem for compressor stations in pipeline networks”. In: *Math. Mech. Complex Syst.* 12.4 (2024), pp. 507–546. DOI: [10.2140/memocs.2024.12.507](https://doi.org/10.2140/memocs.2024.12.507).
- [16] M. Gugat and S. Ulbrich. “Lipschitz Solutions of Initial Boundary Value Problems for Balance Laws”. In: *Math. Models Methods Appl. Sci.* 28.5 (2018), pp. 921–951.
- [17] M. Gugat and D. Wintergerst. “Transient Flow in Gas Networks: Traveling waves”. In: *Int. J. Appl. Math. Comput.* 28.2 (2018), pp. 341–348. DOI: [10.2478/amcs-2018-0025](https://doi.org/10.2478/amcs-2018-0025).
- [18] M. Gugat, R. Schultz, and D. Wintergerst. “Networks of pipelines for gas with non-constant compressibility factor: stationary states”. In: *Comput. Appl. Math.* 37 (2018), pp. 1066–1097. DOI: [10.1007/s40314-016-0383-z](https://doi.org/10.1007/s40314-016-0383-z).
- [19] M. Gugat and M. Schuster. “Stationary Gas Networks with Compressor Control and Random Loads: Optimization with Probabilistic Constraints”. In: *Math. Prob. Eng.* 2018.1 (2018). DOI: [10.1155/2018/7984079](https://doi.org/10.1155/2018/7984079).
- [20] F. Hante. “Mixed-Integer Optimal Control for PDEs: Relaxation via Differential Inclusions and Applications to Gas Network Optimization”. In: *Mathematical Modelling, Optimization, Analytic and Numerical Solutions*. Ed. by P. Manchanda, R. Lozi, and A. Siddiqi. Springer Singapore, 2020, pp. 157–171.
- [21] F. Hante, G. Leugering, A. Martin, L. Schewe, and M. Schmidt. “Challenges in Optimal Control Problems for Gas and Fluid Flow in Networks of Pipes and Canals: From Modeling to Industrial Applications”. In: *Industrial Mathematics and Complex Systems*. Springer, 2017, pp. 77–122.
- [22] S. Kazi, K. Sundar, S. Srinivasan, and A. Zlotnik. “Modeling and optimization of steady flow of natural gas and hydrogen mixtures in pipeline networks”. In: *Int. J. Hydrot. Energy* 54 (2024), pp. 14–24. DOI: [10.1016/j.ijhydene.2023.12.054](https://doi.org/10.1016/j.ijhydene.2023.12.054).
- [23] S. Kazi, K. Sundar, and A. Zlotnik. “Dynamic Optimization and Optimal Control of Hydrogen Blending Operations in Natural Gas Networks”. In: *2024 Americal Control Conference (ACC)*. Institute of Electrical and Electronics Engineers (IEEE), 2024.
- [24] T. Koch, B. Hiller, M. E. Pfetsch, and L. Schewe. *Evaluating Gas Network Capacities*. MOS-SIAM, 2015.
- [25] K. Kumar, G. John, L. Lim, K. Seeger, M. Wakabayashi, and G. Kawamura. *Green Hydrogen in Asia: A Brief Survey of Existing Programmes and Projects*. 2023. URL: <https://www.orrick.com/en/Insights/2023/07/Green-Hydrogen-in-Asia-A-Brief-Survey-of->
- [26] O. Kunz and W. Wagner. “The GERG-2008 Wide-Range Equation of State for Natural Gases and Other Mixtures: An Expansion of GERG-2004”. In: *J. Chem. Eng. Data* 57.11 (2012), pp. 3032–3091. DOI: [10.1021/je300655b](https://doi.org/10.1021/je300655b).

- [27] F. Liers, A. Martin, M. Merkert, N. Mertens, and D. Michaels. “Solving mixed-integer nonlinear optimization problems using simultaneous convexification: a case study for gas networks”. In: *J. Global Optim.* 80 (2021), pp. 307–340. DOI: 10.1007/s10898-020-00974-0.
- [28] J. Málek and O. Souček. “A thermodynamic framework for heatconducting flows of mixtures of two interacting fluids”. In: *J. Appl. Math. Mech.* 102 (2022), Paper No. e202100389.
- [29] A. Nayak and S. Grundel. “Convergence study for composite gas flow in pipes”. In: *Proc. Appl. Math. Mech.* 23 (1 2022), 7 pages. DOI: 10.1002/pamm.202200231.
- [30] M. Schmidt, M. C. Steinbach, and B. M. Willer. “High detail stationary optimization models for gas networks: validation and results”. In: *Optim. Eng.* 17 (2016), pp. 437–472. DOI: 10.1007/s11081-015-9300-3.
- [31] M. Schuster. “Control and Optimization under Uncertainty in the Context of Gas Network Operation”. Habilitation. FAU Erlangen-Nürnberg, Germany, 2026. URL: <https://opus4.kobv.de/opus4-kobv/frontdoor/index/index/docId/410>.
- [32] M. Schuster. “Nodal Control and Probabilistic Constrained Optimization using the Example of Gas Networks”. Dissertation. FAU Erlangen-Nürnberg, Germany, 2021. URL: <https://opus4.kobv.de/opus4-trr154/frontdoor/index/index/docId/410>.
- [33] U.S. Department of Energy, OCED. *Hydrogen: A Flexible Energy Carrier*. 2017. URL: <https://www.energy.gov/cmei/articles/hydrogen-flexible-energy-carrier>.
- [34] U.S. Department of Energy, OCED. *Multi-Year Program Plan*. 2023. URL: <https://www.energy.gov/si>.
- [35] A. Ulke, M. Schuster, and S. Göttlich. “Steady state blended gas flow on networks: Existence and uniqueness of solutions”. In: *Netw. Heterog. Media* 20.3 (2025), pp. 903–937. DOI: 10.3934/nhm.2025039.
- [36] T. Walther and B. Hiller. *Modelling compressor stations in gas networks*. Preprint. Zuse-Institut Berlin (ZIB), 2017. URL: <https://opus4.kobv.de/opus4-trr154/203>.
- [37] D. Wintergerst. “Optimization on Gas Networks under Stochastic Boundary Conditions”. PhD thesis. FAU Erlangen-Nürnberg, Germany, 2019. URL: <https://open.fau.de/handle/openfau/123456789/203>.